



Published in final edited form as:

*Leukemia*. 2022 July ; 36(7): 1907–1915. doi:10.1038/s41375-022-01581-6.

## Ceramide synthase 6 impacts T-cell allogeneic response and graft-versus-host disease through regulating N-RAS/ERK Pathway

M.Hanief Sofi<sup>1,\*</sup>, Linlu Tian<sup>1,2,\*</sup>, Steven Schutt<sup>1</sup>, Imran Khan<sup>3</sup>, Hee-Jin Choi<sup>1,2</sup>, Yongxia Wu<sup>1,2</sup>, David Bastian<sup>1</sup>, Taylor Ticer<sup>1</sup>, Mohamed Faisal Kassir<sup>4</sup>, Firdevs Cansu Atilgan<sup>4</sup>, Jisun Kim<sup>4</sup>, Xiaohui Sui<sup>1</sup>, Aleksandra Zivkovic<sup>5</sup>, Shikhar Mehrotra<sup>6</sup>, John P. O'Bryan<sup>3</sup>, Holger Stark<sup>5</sup>, Paul J. Martin<sup>7</sup>, Besim Ogretmen<sup>4</sup>, Xue-Zhong Yu<sup>1,2,8,#</sup>

<sup>1</sup>Department of Microbiology and Immunology, Medical University of South Carolina, Charleston, SC, USA;

<sup>2</sup>Department of Microbiology and Immunology, Medical College of Wisconsin, Milwaukee, WI, USA;

<sup>3</sup>Department of Cell and Molecular Pharmacology and Experimental Therapeutics, Heinrich Heine University Düsseldorf, Duesseldorf, Germany;

<sup>4</sup>Department of Biochemistry and Molecular Biology, Medical University of South Carolina (MUSC), Heinrich Heine University Düsseldorf, Duesseldorf, Germany;

<sup>5</sup>Institute of Pharmaceutical and Medicinal Chemistry, Heinrich Heine University Düsseldorf, Duesseldorf, Germany;

<sup>6</sup>Department of Surgery, Fred Hutchinson Cancer Research Center, Seattle, WA, USA;

<sup>7</sup>Clinical Research Division, Fred Hutchinson Cancer Research Center, Seattle, WA, USA;

<sup>8</sup>The Cancer Center, Medical College of Wisconsin, Milwaukee, WI, USA.

### Abstract

Allogeneic hematopoietic cell transplantation (allo-HCT) is an effective immunotherapy for various hematologic malignancies, predominantly through potent graft-versus-leukemia (GVL) effect. However, the mortality after allo-HCT is because of relapse of primary malignancy and followed by graft-vs-host-disease (GVHD) as a major cause of transplant-related mortality. Hence, strategies to limit GVHD while preserving the GVL effect are highly desirable. Ceramide,

Users may view, print, copy, and download text and data-mine the content in such documents, for the purposes of academic research, subject always to the full Conditions of use: <https://www.springernature.com/gp/open-research/policies/accepted-manuscript-terms>

<sup>#</sup>Corresponding Author: Dr. Xue-Zhong Yu, MD, MS, Address: 8701 Watertown Plank Road, Milwaukee, WI 53226, USA, Phone: +1 (414) 955-8187, xuyu@mcw.edu.

<sup>\*</sup>Co-first authors, the authors equally contributed to the manuscript

Author contributions

MHS, LT and XZY participated in designing research studies, MHS, SS, IK, HC, YW, DB, TT, MFK, FCA, KJ, and XS participated in conducting experiments and acquiring data. MHS, LT and XZY participated in analyzing and interpreting data and wrote the manuscript. AZ and HS provided ST1072 inhibitor. PJM provided deidentified patient plasma samples and related information and participated in clinical data analysis and interpretation. SM, JO and BO participated in interpreting data and editing the manuscript.

**Disclosure of Conflicts of Interests:** There is no conflict of interest to report.

which serves a central role in sphingolipid metabolism, is generated by ceramide synthases (CerS1–6). In this study, we found that genetic or pharmacologic targeting of CerS6 prevented and reversed chronic GVHD (cGVHD). Furthermore, specific inhibition of CerS6 with ST1072 significantly ameliorated acute GVHD (aGVHD) while preserving the GVL effect, which differed from FTY720 that attenuated aGVHD but impaired GVL activity. At the cellular level, blockade of CerS6 restrained donor T cells from migrating into GVHD target organs and preferentially reduced activation of donor CD4 T cells. At the molecular level, CerS6 was required for optimal TCR signaling, CD3/PKC $\theta$  co-localization, and subsequent N-RAS activation and ERK signaling, especially on CD4<sup>+</sup> T cells. The current study provides rationale and means for targeting CerS6 to control GVHD and leukemia relapse, which would enhance the efficacy of allo-HCT as an immunotherapy for hematologic malignancies in the clinic.

## Introduction

GVHD remains one of the major complications after allo-HCT. aGVHD is distinguished by uncontrolled activation, proliferation and migration of allogeneic donor T cells, as well as their production of pro-inflammatory cytokines in GVHD target organs<sup>11</sup>. In contrast, cGVHD pathogenesis involves several immune cell types, including pathogenic B- and T-cell interactions that result in follicular T helper cell (Tfh) generation. Plasma cell differentiation and autoantibody production have also been demonstrated to contribute to disease pathology<sup>2–4</sup>. Thus, strategies designed to impede the pathogenesis of GVHD by regulating alloreactive donor B and T-cell expansion and inflammatory cytokine production are highly desirable.

The small guanine nucleotide-binding proteins of the Ras family<sup>5</sup>, comprising of the highly homologous H-, N- and K-Ras isoforms in mammals, are rapidly activated after TCR engagement<sup>6, 7</sup>. Each of the 3 mammalian *Ras* genes encodes a membrane-associated 21-kDa protein that acts as a molecular switch to convey extracellularly derived signals into the cell interior. Recently it was reported that CD4<sup>+</sup> T cells lacking N-Ras are intrinsically defective in inducing IFN- $\gamma$  and T-bet early after TCR engagement and exhibit impaired differentiation into Th1 effectors<sup>8</sup>. The Ras/Raf-ERK module reduces the translocation and recruitment of SHP-1 (Src-homology 2 domain (SH2)-containing protein tyrosine phosphatase-1) to the TCR synapse, and sustains and amplifies TCR signaling, leading to inflammation and autoimmunity<sup>8</sup>.

Sphingolipids and their derivatives, particularly ceramide and sphingosine-1-phosphate (S1P), are lipid mediators that regulate varieties of cellular functions including cell growth, survival, and inflammation<sup>9, 10</sup>. It was reported that FTY720 (fingolimod), an oral S1P receptor modulator, antagonizes the activity for all S1PRs except S1PR2 and reduces GVHD while impairing the GVL effect<sup>11</sup>. Likewise, ceramides are also involved in inflammatory processes, as host acid sphingomyelinases (ASMase) have shown to be important for maximal GVHD associated pathology<sup>12</sup>. Recently we and others have also demonstrated that CerS6 deficiency modulates TCR activity, which impacts the development of GVHD and colitis<sup>13, 14</sup>, suggesting that sphingolipids regulate inflammation and GVHD development.

In this study, we targeted CerS6 genetically or pharmacologically and found that these strategies were sufficient to prevent GVHD development. Our collaborators previously reported that ST1072 (*N*-(4-(4-(heptyloxy) phenyl)-1-hydroxy-2-(hydroxymethyl) butan-2-yl)-4-phenylbutanamide) significantly reduces CerS4/6 activity<sup>15</sup>. Our published data indicated that CerS4 in T cells does not play a crucial role in GVHD development<sup>13</sup>, and thus ST1072 is considered as an inhibitor of CerS6. Administration of sphingolipid modulators ST1072 and FTY720 reduced the T-cell alloresponse and GVHD severity, but only ST1072 was able to preserve the GVL activity. The ability of ST1072 to attenuate GVHD and preserve GVL responses was also observed in a human to mouse xenograft model. The increase of plasma ceramides produced by CerS6 also correlated with GVHD development in patients after allo-HCT. Mechanistically we observed that CerS6 was important for optimal TCR mediated N-RAS activity and allogeneic response. The reduced N-RAS activity led to a reduction of its downstream ERK signaling that was associated with restrained ability of T cells to cause GVHD. Overexpression of active N-RAS reduced the impact of CerS6 inhibition and restored T-cell responses. These findings provide a strong rationale and potential means to prevent GVHD while preserving the GVL effect by targeting CerS6 in the clinic.

## Material and Methods

### Mice.

CerS6 KO strain on B6 background<sup>16</sup> was generated by Texas Institute for Genomic Medicine (TIGM). All mice were housed in a pathogen-free facility at the American Association for Laboratory Animal Care–accredited Animal Resource Center at Medical University of South Carolina (MUSC). All animal studies were carried out under protocols approved by the Institutional Animal Care and Use Committee at MUSC. The details about aGVHD, cGVHD, GVL and xenograft GVHD models, and N-RAS activation and transfection in T cells were described as our previous works<sup>13, 17, 18</sup> and in supplemental Material and Methods.

### Human samples.

Serum samples were collected from 37 patients after allo-HCT. Human subject study was approved by Institutional Review Board for Human Research (IRB) at the Fred Hutchinson Cancer Research Center (FHCRC) (protocol #6493). The study was indicated as Not Human Subject Research by the IRB at MUSC. The collaboration between MUSC and FHCRC was conducted under approved Data and Material Transfer and Use Agreement (MTA #200131). HPLC-MS/MS analysis of sphingolipids was operated as previously described<sup>13, 19</sup> and the details were shown in supplemental method.

### Statistics.

For comparison of recipient survival among groups in BMT experiments, the log-rank test was used to determine statistical significance. Clinical scores and body weight loss were compared using a nonparametric Mann-Whitney *U* test. For parametric data, where we use more than two groups, ANOVA was performed. To compare cytokines levels in a two-group analysis, a 2-tailed Student *t* test was performed. To determine the correlation

between the levels of sphingolipids and GVHD development in patients, chi-square and logistic regression analysis were used. These statistics were calculated with SPSS 23.0 and GraphPad Prism software. The variance was similar between the groups that are compared statistically. A p value of <0.05 was considered significant.

## Results

### Inhibition of CerS6 reduces the T-cell response to alloantigen.

Using a genetic approach, we previously demonstrated that CerS6 promotes T-cell responses to alloantigen and thus GVHD development<sup>13</sup>. To translate the fundamental discovery towards clinical application, we aimed to block CerS6 via a pharmacological approach by testing a novel CerS6/S4 inhibitor (ST1072)<sup>20</sup> in murine models of allogeneic bone marrow transplantation (BMT). We first tested the effect of ST1072 on T-cell expansion and activation with a range of doses *in vivo*. While the inhibition of CerS6 did not affect T-cell expansion based on percentage of donor T cells and CFSE dilution, it reduced IFN- $\gamma$  production of donor T cells in a dose-dependent manner (S. Fig. 1A–B). Given that systemic treatment affects other cells besides donor T cells, we asked how inhibition of CerS6 affected antigen-presenting cells (APCs). Indeed, ST1072 treatment significantly reduced the expression of costimulatory molecules CD40 and CD86 on donor B cells, DCs and macrophages in recipients (S. Fig. 1C), which would limit antigen-processing function of various APCs. Taken together, these results indicate that ST1072 inhibits CerS6 and the inhibition of CerS6 systemically reduces the activation of lymphocytes and myeloid cells in allogeneic recipients.

### ST1072 is effective in the prevention and treatment of cGVHD after allo-BMT.

—To verify *in vivo* inhibition of CerS6 with ST1072, we did lipidomic analyses on sphingosine lipids in recipient sera, and observed that ST1072 treatment selectively reduced C<sub>16</sub> ceramide, a main product of CerS6 (Fig. 1A). Because the treatment with ST1072 inhibited both T- and B-cell activation that contribute to the development of cGVHD, we evaluated the effect of ST1072 on cGVHD with CerS6 knock-out (KO) donors as controls. In an MHC-mismatched BMT model with aGVHD to cGVHD<sup>21, 22</sup> transition feature (B6 → BALB/c), the treatment of recipients with ST1072 as prophylaxis significantly reduced the severity of cGVHD reflected by body weight loss and clinical manifestations (Fig. 1B.). In fact, the severity of cGVHD in the recipients transplanted with WT graft and treated with ST1072 was similar to that in the recipients transplanted with CerS6 KO graft. The finding was extended to an MHC-matched BMT model with a sclerodermatous cGVHD feature (B10.D2 → BALB/c) (S. Fig. 2A–B). ST1072 improved clinical conditions of mice during cGVHD development as shown by the recipient images taken on day 60 post-BMT (S. Fig. 2A). To address whether this intervention could treat established cGVHD, we started ST1072 at 28 days after allo-BMT and found that such delayed treatment with ST1072 also significantly reduced cGVHD severity (S. Fig. 2C). These results indicate that targeting CerS6 pharmacologically can prevent cGVHD development or even treat established cGVHD

**CerS6 modulates B- and T-cell function during cGVHD development.**—We next assessed the impact of ST1072 on donor T- and B-cell responses after BMT. Either early or late treatment with ST1072 markedly reduced splenic T follicular helper (Tfh) cells with a significant increase in T follicular regulatory (Tfr) cells in the MHC-matched BMT model (S. Fig. 3A–B). Early or late ST1072 administration also significantly inhibited the production of IFN- $\gamma$  by donor CD4 but not CD8 T cells in the recipient spleens and peripheral lymph nodes (LNs) (Fig. 2A–B, S. Fig. 3C). Moreover, the inhibition of CerS6 with ST1072 preserved B cells, but significantly reduced percentages of germinal center B cells (GC, Fas<sup>+</sup>GL7<sup>+</sup>) and plasma cells (CD138<sup>+</sup>B220<sup>low</sup>) (Fig. 2C, S. Fig. 3D). In the MHC-mismatched BMT model, CerS6 inhibition with ST1072 significantly enhanced T-cell reconstitution in recipient thymus reflected by the percentage of CD4<sup>+</sup>CD8<sup>+</sup> double-positive (DP) cells, which was similar to the recipient with CerS6 deficient donor graft (S. Fig. 4A–B). We also observed that CerS6 inhibition also significantly reduced Th1 response (S. Fig. 4C), improved B-cell reconstitution, and decreased pathogenic B-cell differentiation (S. Fig. 4D). These results suggest that ST1072 administration alleviates cGVHD severity and improves reconstitution of recipient thymocytes through reducing cytokine production by donor CD4 T cells and the activation and pathogenesis of donor B cells.

**ST1072 treatment alleviates GVHD without impairing the GVL activity.**—

Previous reports have shown that FTY720 suppresses the migration of pathogenic T cells to target organs and thus prevents aGVHD progression<sup>23</sup>. However, FTY720 also impairs GVL effect against C1498, a myeloid leukemia<sup>11</sup>. Given that CerS6 KO T cells reduce the ability to induce GVHD while preserving the GVL effect<sup>13</sup>, we hypothesized that inhibition of CerS6 with ST1072 would maintain the GVL effect. Using an MHC-mismatched BMT model (B6→BALB/c), we first compared the impact of ST1072 and FTY720 side-by-side in GVHD development. Treatment with ST1072 or FTY720 significantly attenuated GVHD reflected by recipient clinical score and survival (S. Fig. 5A–B). To evaluate the impact of ST1072 on the GVL effect, we utilized mixed-lineage leukemia (MLL) (Fig. 3A–C) and chronic myeloid leukemia (CML) in (B6→BALB/c) BMT models (S. Fig. 6A–C). The recipients treated with ST1072 were free from MLL or CML whereas majority of those with FTY720 died from leukemia relapse (Fig. 3C, S. Fig. 5C–D, 6C). To substantiate our findings, we tested one additional MHC-matched BMT model (C3H.SW→B6) with C1498 that was previously tested for FTY720<sup>11</sup>, and we further validated the effect of ST1072 on GVH/GVL response (S. Fig. 7A–C). Taken all together, these results from 3 different models indicate that while treatment with ST1072 or FTY720 significantly attenuated GVHD severity, only ST1072 preserved the GVL effect.

**ST1072 regulates T-cell expansion and migration.**—Development of GVHD requires donor T-cell expansion in lymphoid organs and migration into target organs<sup>13, 14</sup>. Here we found that treatment with ST1072 significantly increased absolute numbers of donor CD4 and CD8 T cells in recipient spleens (secondary lymphoid organ) but decreased them in livers (GVHD target organ) (S. Fig. 8A, C). Given percentages and the absolute numbers of IFN- $\gamma$ -producing T cells were increased in recipient spleens (S. Fig. 8A–B). The percentages of IL-4<sup>+</sup> or Foxp3<sup>+</sup> cells were similar among donor CD4 T cells (S. Fig. 8B), but absolute numbers of these cells were significantly increased in recipient spleens after

treatment with ST1072 (S. Fig. 8A). In contrast, a significantly lower number of IFN- $\gamma$ - and IL-4-producing donor T cells were found in recipient livers after ST1072 treatment (S. Fig. 8C–D). Given donor T cells accumulated in recipient spleens while decreased in the livers, we hypothesized that ST1072 might reduce T-cell migration to GVHD target organs. CXCR3 and CCR5 contribute to donor T-cell infiltration into GVHD target organs, including gastrointestinal tract (GI), skin, liver and lung. Eliminating CCR6, CCR9 and  $\alpha 4\beta 7$  integrin expression from donor T-cell result in reduced migration of T cells into GI tract. CCR4 and CCR6 are required for T-cell trafficking into skin system<sup>24</sup>. Indeed, ST1072 administration significantly reduced the expression of CXCR3, CCR5, CCR6 and CCR9 but not  $\alpha 4\beta 7$  on donor T cells in recipient spleens (S. Fig. 8E, 9A) and decreased the numbers of donor T cells that migrated into recipient intestines and livers (S. Fig. 9B). To test the impact of ST1072 more directly in T-cell expansion and/or migration, we transferred  $\beta$ -actin luciferase transgenic T cells from B6 donors into irradiated allogeneic recipients and followed donor T-cell distribution and accumulation using bioluminescent imaging (BLI) on 7, 14 and 20 days post-BMT (Fig. 4A–B). While the BLI intensity in whole body (Fig. 4A) and mesenteric LN was comparable, the intensity was preferentially reduced in spleen and GVHD target organs including gut and lung but not liver (Fig. 4B–C, S. Fig. 8F), suggesting that inhibition of CerS6 reduced T-cell expansion and migration into GVHD target organs.

**The role of ST1072 in proximal TCR signaling.**—TCR signaling dictates T-cell response to cognate antigen. Previously we showed that CerS6 affects T-cell activation and function by regulating early TCR signaling<sup>13</sup>. To further understand how CerS6 affects signaling molecules in T-cell membranes, we labeled cell surface proteins with biotin and examined pulldown biotin-labeled molecules before or after TCR stimulation *in vitro*. All pulled-down proteins isolated from WT, CerS6KO T cells, or WT T cells plus ST1072 were separated in SDS-PAGE gel and displayed by silver staining. Different protein expressions among these samples were apparent in a few areas, particularly in 20–50 kD proteins (data not shown). We then retrieved the proteins between 20 and 50 kD from the gel and identified them using mass spectrometry. Among these proteins, we found that GTPase N-Ras, Ras GTPase-activating protein-binding protein 2 (G3BP2), and 14-3-3 $\epsilon$  were present in WT but absent in CerS6KO T cells or WT T cells exposed to ST1072. Zap-70 has been shown to mediate RasGRP1 membrane localization and lead to N-Ras activation<sup>25</sup> and N-Ras acts as a critical controller of Th1 responses, primarily by transmitting TCR signals for Th1 priming of CD4 T cells<sup>8, 26</sup>. We therefore chose to study further how CerS6/C16-Cer regulates N-Ras activation. When CerS6 was absent (CerS6 KO) or inhibited (WT + ST1072), T cells failed to upregulate N-Ras or activate ERK after TCR stimulation (Fig. 5A). Among Ras GTPases, only N-Ras, not K-Ras or H-Ras, was affected by CerS6, and the reduction of membrane N-Ras was more apparent than cytosol N-Ras when CerS6 was inhibited (Fig. 5B and data not shown). We hypothesized that the lack of membrane-associated N-RAS is responsible for the impairment of T-cell activation when CerS6 is inhibited or absent. To address this question, we transduced naïve T cells with active N-Ras plasmid and confirmed the expression of active N-Ras as reflected by HA-tag staining (S. Fig. 10A). As expected, ST1072 treatment significantly reduced IFN- $\gamma$  production in control CD4 T cells but did not affect CD4 T cells transduced with active N-Ras (S. Fig. 10B, Fig. 5C). Taken together,

these data indicate that CerS6 or C16-ceramide regulates T-cell allogeneic responses through N-RAS activation.

**CerS6 KO impacts CD3 and PKC $\theta$  capping differently in CD4 and CD8 T cells after TCR engagement.**—PKC $\theta$  is the only T cell-expressed PKC isoforms that localizes selectively to the center of the immunological synapse (IS) following conventional T cell antigen stimulation<sup>13, 27, 28</sup> and contacts between T cells and APCs<sup>29</sup>, which can induce activation of ERK<sup>30, 31</sup>. Our previous data indicated that CerS6 played a more important role in CD4 than in CD8 T cells, thus we asked if CerS6 affects PKC $\theta$  expression and co-localization with the TCR differently between CD4 and CD8 T cells. Upon stimulation with TCR crosslinking, PKC $\theta$  expression and co-localization with CD3 were severely impaired in CerS6KO CD4 T cells as compared with the WT counterparts (Fig. 6). In contrast, CerS6 deficiency had little or no effect on CD8 T cells (S. Fig. 11). These data indicate that CerS6 KO preferentially affects CD4 T-cell activation and function by regulating early TCR signaling.

**The effects of ST1072 on human T-cell mediated GVH/GVL responses in xenograft transplant model.**—For translational purposes we sought to further test the impact of ST1072 on human GVHD using a xenograft GVHD model. We transplanted HLA-A2<sup>-</sup> human PBMCs into irradiated NSG-A2<sup>+</sup> mice and treated these recipient mice with vehicle or ST1072. Evidently, treatment with ST1072 significantly reduced GVHD severity (Fig. 7A). To further assess the impact of ST1072 in the GVL activity, we set up the transplant similarly to figure 7A and infused Raji lymphoma into the recipients (Fig. 7B). As expected, all the recipients of Raji lymphoma without human PBMCs died from leukemia relapse within 30 days after BMT. In contrast, the recipients transferred with PBMCs and treated with vehicle control died from GVHD, reflected by 90% lethality, severe clinical score and no tumor signal. In contrast, ST1072 treatment rescued 40–50% recipients from GVHD lethality and the survived recipients were free from tumor relapse (Fig. 7B). These data indicate that ST1072 treatment attenuates GVHD while preserving the GVL activity mediated by human T cells.

We next evaluated the effects of ST1072 on human T-cell responses *in vivo*. On day 14 after transplant, we examined the presence of donor T cells in recipient spleens and livers (S. Fig. 12A–B). Treatment of ST1072 significantly decreased numbers of CD3<sup>+</sup> T cells both in the spleen and liver (S. Fig. 12D–F), while increasing the frequency of Tregs in both organs (S. Fig. 12A–C, E). Furthermore, ST1072 also significantly reduced the number and frequency of IFN- $\gamma$ -producing T cells in the liver (S. Fig. 12E–F). These data indicate that ST1072 treatment can reduce T-cell activation, differentiation, and migration.

Finally, we asked whether sphingolipid metabolites are associated with GVHD development in human patients. To address this question, we obtained patient plasma samples that were collected at Fred Hutch under protocol #6493<sup>32, 33</sup>. The levels of sphingolipids were analyzed with mass spectrophotometry in plasma samples from 20 patients with GVHD and 17 without GVHD 14 days after allogeneic HCT. The basslines were comparable between these two groups of patients<sup>34</sup>, except those patients with GVHD were younger than those without GVHD (S. Table 1A). There was also no significant difference in patient

characteristics associated with allogeneic HCT between these two groups (S. Table 1A–B). We observed that the levels of C14-, C16- and C26-Ceramide as well as dhSphingosine-1P (dhSph-1P) and Sph-1P were higher in the patients with GVHD than those without GVHD (Table 1). Nevertheless, the data from chi-square and logistic regression analysis revealed that only C16-Ceramide, dhSph-1P and Sph-1P displayed a positive correlation with gut, liver and overall but not skin GVHD development (S. Table 2 and Table 1). These results suggest that C16-ceramide metabolism may contribute to GVHD pathogenesis in human.

## Discussion

CerS6, which preferentially generates C<sub>16</sub>-ceramide, has been implicated to play roles in various cellular responses<sup>35</sup>. In the current study, we evaluated the therapeutic potential of a new CerS6 inhibitor, ST1072. Administration of ST1072 not only reduced C<sub>16</sub>-ceramide generation, T-cell allogeneic responses, and GVHD severity, but also preserved the GVL responses both in mouse and xenograft transplant models. Moreover, treatment with ST1072 up to 2 mg/kg did not cause additional weight loss or impairment of bone marrow reconstitution as compared to vehicle control (data not shown), indicating that less than 2 mg/kg ST1072 presented little or no toxicity while it was efficacious in the prevention of GVHD. The increase in C16 ceramide was also observed in GVHD patient serum samples 14 days post-HCT, suggesting a possible role of C<sub>16</sub>-ceramide in GVHD development. Mechanistically, treatment with ST1072 restrained the ability of donor T cells to activate and migrate to target organs in allogeneic recipients. Furthermore, CerS6 was required for TCR-mediated N-RAS activity, by genetically or pharmacologically reducing CerS6, this effect of N-RAS on type I T-cell response could be reversed (S. Fig. 13).

B cells contribute to GVHD pathogenesis partially through presenting alloantigen to T cells<sup>36, 37</sup>. CerS6 plays pleiotropic roles in regulating the differentiation and function of multiple immune cells including B and T cells<sup>38</sup>. These immune cells play a significant role in the pathogenesis of cGVHD by enhancing Th1, Tfh, germinal center (GC) B cells, and plasma cells (PC)<sup>39</sup>. Tfh is a pathogenic T-cell subset that contributes to cGVHD pathogenesis<sup>3, 40</sup> and well-known to provide essential signals to support GC, memory B cells or antibody-producing PC development<sup>41–43</sup>. We demonstrated that prophylactic administration of ST1072 significantly ameliorated cGVHD severity in both MHC-matched and MHC-mismatched cGVHD models with minimal toxicity (Fig. 1B, S. Fig. 2A–B). Furthermore, treatment with ST1072 was able to halt further development of established cGVHD (S. Fig. 2C). Consistent with donor T- and B-cell pathogenesis, treatment with ST1072 significantly reduced Tfh cells, GC B-cells, and PC development.

Imaging and survival studies indicate that FTY720 impairs the GVL response against a myeloid leukemia<sup>11</sup>. These observations highlight the limitation of FTY720 as a therapeutic agent where allo-HCT is applied as an immunotherapy for hematological malignancy. Unlike FTY720, ST1072 preserved the GVL effect against MLL (Fig. 3C, S. Fig. 5C–D). The potential of ST1072 in the preservation of the GVL effect has been substantiated in other malignant models including CML (S. Fig. 6), acute leukemia (S. Fig. 7), and human B-cell lymphoma (Fig. 7B). Given selective GVL effect depends on magnitude and diversity of the alloreactive T cell response<sup>44</sup>, we reason that the preservation of GVL activity



upon CerS6 blockade can be generalized across a variety of allogeneic T-cell responses to hematological malignancies. We attribute the preserved GVL effect of ST1072 to the largely intact activation and function of CD8 cytotoxic T lymphocytes upon pharmacological blockade of CerS6. There are several lines of evidence to support the outcome: 1) although donor CD8 T cells from ST1072 treated mice showed decreased pro-inflammatory response in the early phase of BMT (S. Fig. 1), their expansion and activation were not compromised in the later phase of BMT (Fig. 4, S. Fig. 8, 9); 2) treatment with ST1072 significantly reduced migration of donor T cells into target organs (e.g. liver), whereas it did not impact T-cell expansion or cytokine production in the lymphoid organs (Fig. 4, S. Fig. 8A–B); and 3) impaired co-localization of CD3/PKC $\theta$  in CerS6 KO CD4 T cells but not CD8 T cells upon TCR stimulation (Fig. 6, S. Fig. 11); 4) compared with CD8 T cells, CD4 T cells are more sensitive to CerS6-mediated N-RAS/ERK activation (Fig. 5).

Donor T-cell activation in GVHD recipients is influenced by the TCR signal, cytokines, and chemokines which are required for full T-cell activation and migration towards target tissues<sup>45</sup>. Here we observed that CerS6 is required for TCR proximal signaling on CD4 but not CD8 T cells (Fig. 6, S. Fig. 11). TCR signaling upregulates small G-protein Ras<sup>46</sup>, which in turn activates signal-regulated kinases, ERK1/2 phosphorylation through Raf-MAPK dependent pathway<sup>46</sup>. Increased ERK phosphorylation leads to inflammation and autoimmunity<sup>47</sup>. Published reports showed that C16 ceramide selectively enhances the association of Raf-1 with Ras-GTP<sup>48</sup>, suggesting that the interaction is important for downstream signaling<sup>49</sup>. Previously it was reported that N-Ras dependent pathways are required for optimal TCR-mediated IFN- $\gamma$  induction<sup>8</sup>. In the current study, mass spectrometry and biochemical analysis confirm that CerS6 is needed to active of N-Ras as genetic deletion or pharmacological inhibition of CerS6 decreases its activity. Decreased N-Ras activity leads to reduced ERK activation and T-cell allogeneic responses. Furthermore, overexpression of active N-Ras reduced the impact of ST1072 and restored Th1 response. Thus, CerS6 regulates T-cell allogeneic response and GVHD pathogenicity through N-Ras/ERK axis.

In the current study, we have demonstrated that CerS6 can be targeted pharmacologically, and blockade of CerS6 is efficacious in the prevention of aGVHD and cGVHD. Furthermore, the blockade of CerS6 preserved the GVL effect against several types of leukemia and lymphoma. These benefits from CerS6 inhibition are likely due to a dominant role of CerS6 in the regulation of donor CD4 T-cell responses to alloantigen through N-RAS/ERK pathway, which is not required for alloreactivity of CD8 T cells. Our study provides a strong rationale and novel means to therapeutically target CerS6 in controlling GVHD and leukemia relapse for patients undergoing allogeneic HCT. However, the precise mechanisms how CerS6 regulates CD8 T-cell anti-tumor immunity requires further investigation. More patient samples at various time points will likely be required for further validating sphingolipid metabolites as risk factors for GVHD development.

## Supplementary Material

Refer to Web version on PubMed Central for supplementary material.

## Acknowledgments

We would also like to thank the Flow Cytometry Core, Small Animal Imaging Core, Lipidomics Shared Resources and Cell & Molecular Imaging Facilities at Medical University of South Carolina for the assistance. This work is supported in part by SC SmartState Cancer Stem Cell Biology & Therapy Program and by R01 grants from the National Institutes of Health including AI118305 and HL140953 (X.-Z.Y.); CA214641, DE016572, P01 CA203628, and SC SmartState Endowment in Lipidomics and Drug Discovery (B.O.); and the DFG GRK2158 (H.S.)

## Data Availability Statement:

All the data in this research are available.

## References

1. Zeiser R, Blazar BR. Acute Graft-versus-Host Disease - Biologic Process, Prevention, and Therapy. *N Engl J Med* 2017 Nov 30; 377(22): 2167–2179. [PubMed: 29171820]
2. Srinivasan M, Flynn R, Price A, Ranger A, Browning JL, Taylor PA, et al. Donor B-cell alloantibody deposition and germinal center formation are required for the development of murine chronic GVHD and bronchiolitis obliterans. *Blood* 2012 Feb 9; 119(6): 1570–1580. [PubMed: 22072556]
3. Flynn R, Du J, Veenstra RG, Reichenbach DK, Panoskaltis-Mortari A, Taylor PA, et al. Increased T follicular helper cells and germinal center B cells are required for cGVHD and bronchiolitis obliterans. *Blood* 2014 Jun 19; 123(25): 3988–3998. [PubMed: 24820310]
4. Daenthanasamak A, Iamsawat S, Chakraborty P, Nguyen HD, Bastian D, Liu C, et al. Targeting Sirt-1 controls GVHD by inhibiting T-cell allo-response and promoting Treg stability in mice. *Blood* 2019 Jan 17; 133(3): 266–279. [PubMed: 30514750]
5. Olson MF, Marais R. Ras protein signalling. *Seminars in immunology* 2000 Feb; 12(1): 63–73. [PubMed: 10723799]
6. Ehrhardt A, David MD, Ehrhardt GR, Schrader JW. Distinct mechanisms determine the patterns of differential activation of H-Ras, N-Ras, K-Ras 4B, and M-Ras by receptors for growth factors or antigen. *Molecular and cellular biology* 2004 Jul; 24(14): 6311–6323. [PubMed: 15226433]
7. Mor A, Campi G, Du G, Zheng Y, Foster DA, Dustin ML, et al. The lymphocyte function-associated antigen-1 receptor costimulates plasma membrane Ras via phospholipase D2. *Nature cell biology* 2007 Jun; 9(6): 713–719. [PubMed: 17486117]
8. Iborra S, Soto M, Stark-Aroeira L, Castellano E, Alarcon B, Alonso C, et al. H-ras and N-ras are dispensable for T-cell development and activation but critical for protective Th1 immunity. *Blood* 2011 May 12; 117(19): 5102–5111. [PubMed: 21444916]
9. Kunkel GT, Maceyka M, Milstien S, Spiegel S. Targeting the sphingosine-1-phosphate axis in cancer, inflammation and beyond. *Nature reviews Drug discovery* 2013 Sep; 12(9): 688–702. [PubMed: 23954895]
10. Schneider G, Sellers ZP, Bujko K, Kakar SS, Kucia M, Ratajczak MZ. Novel pleiotropic effects of bioactive phospholipids in human lung cancer metastasis. *Oncotarget* 2017 Aug 29; 8(35): 58247–58263. [PubMed: 28938552]
11. Taylor PA, Ehrhardt MJ, Lees CJ, Tolar J, Weigel BJ, Panoskaltis-Mortari A, et al. Insights into the mechanism of FTY720 and compatibility with regulatory T cells for the inhibition of graft-versus-host disease (GVHD). *Blood* 2007 Nov 1; 110(9): 3480–3488. [PubMed: 17606761]
12. Rotolo JA, Stancevic B, Lu SX, Zhang J, Suh D, King CG, et al. Cytolytic T cells induce ceramide-rich platforms in target cell membranes to initiate graft-versus-host disease. *Blood* 2009 Oct 22; 114(17): 3693–3706. [PubMed: 19666872]
13. Sofi MH, Heinrichs J, Dany M, Nguyen H, Dai M, Bastian D, et al. Ceramide synthesis regulates T cell activity and GVHD development. *JCI Insight* 2017 May 18; 2(10).
14. Scheffel MJ, Helke K, Lu P, Bowers JS, Ogretmen B, Garrett-Mayer E, et al. Adoptive Transfer of Ceramide Synthase 6 Deficient Splenocytes Reduces the Development of Colitis. *Sci Rep* 2017 Nov 14; 7(1): 15552. [PubMed: 29138469]

15. Schiffmann S, Hartmann D, Fuchs S, Birod K, Ferreiròs N, Schreiber Y, et al. Inhibitors of specific ceramide synthases. *Biochimie* 2012 Feb; 94(2): 558–565. [PubMed: 21945810]
16. Ebel P, Vom Dorp K, Petrasch-Parwez E, Zlomuzica A, Kinugawa K, Mariani J, et al. Inactivation of ceramide synthase 6 in mice results in an altered sphingolipid metabolism and behavioral abnormalities. *The Journal of biological chemistry* 2013 Jul 19; 288(29): 21433–21447. [PubMed: 23760501]
17. Sofi MH, Wu Y, Schutt SD, Dai M, Daenthanasanmak A, Heinrichs Voss J, et al. Thioredoxin-1 confines T cell alloresponse and pathogenicity in graft-versus-host disease. *J Clin Invest* 2019 May 2; 129(7): 2760–2774. [PubMed: 31045571]
18. Taylor SJ, Resnick RJ, Shalloway D. Nonradioactive determination of Ras-GTP levels using activated ras interaction assay. *Methods Enzymol* 2001; 333: 333–342. [PubMed: 11400349]
19. Bielawski J, Pierce JS, Snider J, Rembiesa B, Szulc ZM, Bielawska A. Sphingolipid analysis by high performance liquid chromatography-tandem mass spectrometry (HPLC-MS/MS). *Adv Exp Med Biol* 2010; 688: 46–59. [PubMed: 20919645]
20. Schiffmann S, Hartmann D, Fuchs S, Birod K, Ferreiros N, Schreiber Y, et al. Inhibitors of specific ceramide synthases. *Biochimie* 2012 Feb; 94(2): 558–565. [PubMed: 21945810]
21. Schroeder MA, DiPersio JF. Mouse models of graft-versus-host disease: advances and limitations. *Dis Model Mech* 2011 May; 4(3): 318–333. [PubMed: 21558065]
22. Wu T, Young JS, Johnston H, Ni X, Deng R, Racine J, et al. Thymic damage, impaired negative selection, and development of chronic graft-versus-host disease caused by donor CD4+ and CD8+ T cells. *J Immunol* 2013 Jul 1; 191(1): 488–499. [PubMed: 23709681]
23. Ryu J, Jhun J, Park MJ, Baek JA, Kim SY, Cho KH, et al. FTY720 ameliorates GvHD by blocking T lymphocyte migration to target organs and by skin fibrosis inhibition. *J Transl Med* 2020 Jun 6; 18(1): 225. [PubMed: 32505218]
24. Wysocki CA, Panoskaltis-Mortari A, Blazar BR, Serody JS. Leukocyte migration and graft-versus-host disease. *Blood* 2005 Jun 1; 105(11): 4191–4199. [PubMed: 15701715]
25. Kremer KN, Kumar A, Hedin KE. G alpha i2 and ZAP-70 mediate RasGRP1 membrane localization and activation of SDF-1-induced T cell functions. *Journal of immunology* 2011 Sep 15; 187(6): 3177–3185.
26. Lynch SJ, Zavadil J, Pellicer A. In TCR-stimulated T-cells, N-ras regulates specific genes and signal transduction pathways. *PloS one* 2014; 8(6): e63193. [PubMed: 23755101]
27. Zhang EY, Kong KF, Altman A. The yin and yang of protein kinase C-theta (PKCθ): a novel drug target for selective immunosuppression. *Adv Pharmacol* 2013; 66: 267–312. [PubMed: 23433459]
28. Monks CR, Kupfer H, Tamir I, Barlow A, Kupfer A. Selective modulation of protein kinase C-theta during T-cell activation. *Nature* 1997 Jan 2; 385(6611): 83–86. [PubMed: 8985252]
29. Bi K, Tanaka Y, Coudronniere N, Sugie K, Hong S, van Stipdonk MJ, et al. Antigen-induced translocation of PKC-theta to membrane rafts is required for T cell activation. *Nature immunology* 2001 Jun; 2(6): 556–563. [PubMed: 11376344]
30. López-Huertas MR, Li J, Zafar A, Rodríguez-Mora S, García-Domínguez C, Mateos E, et al. PKCθ and HIV-1 Transcriptional Regulator Tat Co-exist at the LTR Promoter in CD4(+) T Cells. *Front Immunol* 2016; 7: 69. [PubMed: 26973648]
31. Byerly J, Halstead-Nussloch G, Ito K, Katsyv I, Irie HY. PRKCQ promotes oncogenic growth and anoikis resistance of a subset of triple-negative breast cancer cells. *Breast Cancer Res* 2016 Sep 23; 18(1): 95. [PubMed: 27663795]
32. Martin PJ, Rizzo JD, Wingard JR, Ballen K, Curtin PT, Cutler C, et al. First- and second-line systemic treatment of acute graft-versus-host disease: recommendations of the American Society of Blood and Marrow Transplantation. *Biology of blood and marrow transplantation : journal of the American Society for Blood and Marrow Transplantation* 2012 Aug; 18(8): 1150–1163.
33. Martin PJ, Inamoto Y, Flowers ME, Carpenter PA. Secondary treatment of acute graft-versus-host disease: a critical review. *Biology of blood and marrow transplantation : journal of the American Society for Blood and Marrow Transplantation* 2012 Jul; 18(7): 982–988.
34. Bastian D, Sui X, Nguyen HD, Wu Y, Schutt S, Tian L, et al. Interleukin-23 receptor signaling by interleukin-39 potentiates T cell pathogenicity in acute graft-versus-host disease. *American journal*

of transplantation : official journal of the American Society of Transplantation and the American Society of Transplant Surgeons 2021 May 2.

35. Wegner MS, Schiffmann S, Parnham MJ, Geisslinger G, Grosch S. The enigma of ceramide synthase regulation in mammalian cells. *Progress in lipid research* 2016 Jul; 63: 93–119. [PubMed: 27180613]
36. Wu Y, Schutt S, Paz K, Zhang M, Flynn RP, Bastian D, et al. MicroRNA-17–92 is required for T-cell and B-cell pathogenicity in chronic graft-versus-host disease in mice. *Blood* 2018 Apr 26; 131(17): 1974–1986. [PubMed: 29530952]
37. Young JS, Wu T, Chen Y, Zhao D, Liu H, Yi T, et al. Donor B cells in transplants augment clonal expansion and survival of pathogenic CD4+ T cells that mediate autoimmune-like chronic graft-versus-host disease. *Journal of immunology* 2012 Jul 1; 189(1): 222–233.
38. Schiffmann S, Ferreiros N, Birod K, Eberle M, Schreiber Y, Pfeilschifter W, et al. Ceramide synthase 6 plays a critical role in the development of experimental autoimmune encephalomyelitis. *J Immunol* 2012 Jun 1; 188(11): 5723–5733. [PubMed: 22544924]
39. Schutt SD, Wu Y, Tang CH, Bastian D, Nguyen H, Sofi MH, et al. Inhibition of the IRE-1alpha/XBP-1 pathway prevents chronic GVHD and preserves the GVL effect in mice. *Blood advances* 2018 Feb 27; 2(4): 414–427. [PubMed: 29483082]
40. Forcade E, Kim HT, Cutler C, Wang K, Alho AC, Nikiforow S, et al. Circulating T follicular helper cells with increased function during chronic graft-versus-host disease. *Blood* 2016 May 19; 127(20): 2489–2497. [PubMed: 26944544]
41. Craft JE. Follicular helper T cells in immunity and systemic autoimmunity. *Nature reviews Rheumatology* 2012 May 1; 8(6): 337–347. [PubMed: 22549246]
42. Weinstein JS, Herman EI, Lainez B, Licona-Limon P, Esplugues E, Flavell R, et al. TFH cells progressively differentiate to regulate the germinal center response. *Nature immunology* 2016 Oct; 17(10): 1197–1205. [PubMed: 27573866]
43. Crotty S T follicular helper cell differentiation, function, and roles in disease. *Immunity* 2014 Oct 16; 41(4): 529–542. [PubMed: 25367570]
44. van Bergen CA, van Luxemburg-Heijs SA, de Wreede LC, Eefting M, von dem Borne PA, van Balen P, et al. Selective graft-versus-leukemia depends on magnitude and diversity of the alloreactive T cell response. *J Clin Invest* 2017 Feb 1; 127(2): 517–529. [PubMed: 28067665]
45. Zeiser R, Socie G, Blazar BR. Pathogenesis of acute graft-versus-host disease: from intestinal microbiota alterations to donor T cell activation. *British journal of haematology* 2016 Oct; 175(2): 191–207. [PubMed: 27619472]
46. Soares-Silva M, Diniz FF, Gomes GN, Bahia D. The Mitogen-Activated Protein Kinase (MAPK) Pathway: Role in Immune Evasion by Trypanosomatids. *Frontiers in microbiology* 2016; 7: 183. [PubMed: 26941717]
47. Singh K, Deshpande P, Pryshchep S, Colmegna I, Liarski V, Weyand CM, et al. ERK-dependent T cell receptor threshold calibration in rheumatoid arthritis. *Journal of immunology* 2009 Dec 15; 183(12): 8258–8267.
48. Muller G, Storz P, Bourteele S, Doppler H, Pfizenmaier K, Mischak H, et al. Regulation of Raf-1 kinase by TNF via its second messenger ceramide and cross-talk with mitogenic signalling. *The EMBO journal* 1998 Feb 2; 17(3): 732–742. [PubMed: 9450998]
49. Lu SX, Alpdogan O, Lin J, Balderas R, Campos-Gonzalez R, Wang X, et al. STAT-3 and ERK 1/2 phosphorylation are critical for T-cell alloactivation and graft-versus-host disease. *Blood* 2008 Dec 15; 112(13): 5254–5258. [PubMed: 18838616]

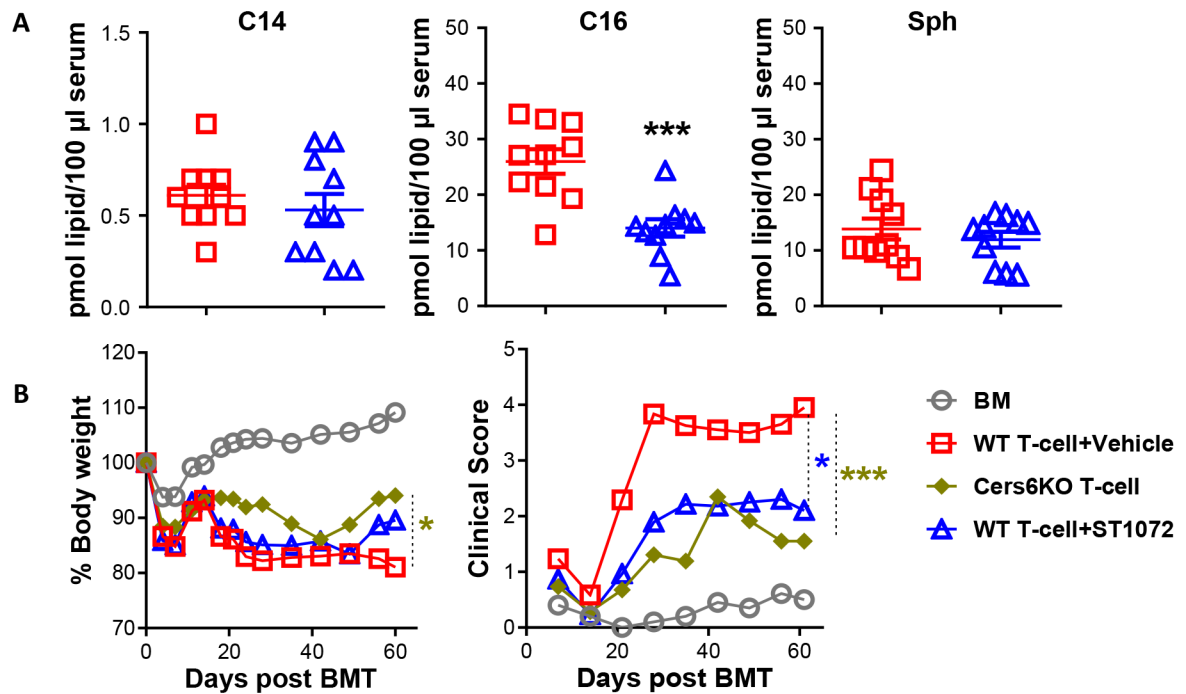


**Figure 1. Absence of CerS6 on donor T cells or inhibition of CerS6 ameliorates cGVHD development.**

(A) The splenocytes from WT mice on B6 background were intravenously (i.v.) injected at  $6 \times 10^6$ /mouse into lethally irradiated BALB/c mice. The recipient mice were injected with vehicle or ST1072 at 1mg/kg intraperitoneally (i.p.) from day -1 to day 3. Four days after cell transfer, serum was collected and subjected to mass spectrometry HPLC-MS analysis for different ceramide species. Data shown is pooled from two independent experiments (n=10 per group). BALB/c mice were lethally irradiated and transplanted with  $5 \times 10^6$ /mouse T-cell depleted-bone marrow (TCD-BM) alone or plus splenocytes ( $0.5 \times 10^6$ /mouse) either from WT or CerS6KO B6 mice. One group of WT recipient mice was injected i.p. with ST1072 at 2 mg/kg from day-1 to day 28. The recipients were monitored for body weight and clinical score (B) until 60 days post-BMT. Data shown is from two combined experiments (N=10–15 per group). Recipient clinical scores and body weight loss were compared using a nonparametric Mann-Whitney *U* test. Asterisks indicate statistical significance \**p* < 0.05, \*\*\**p* < 0.001.

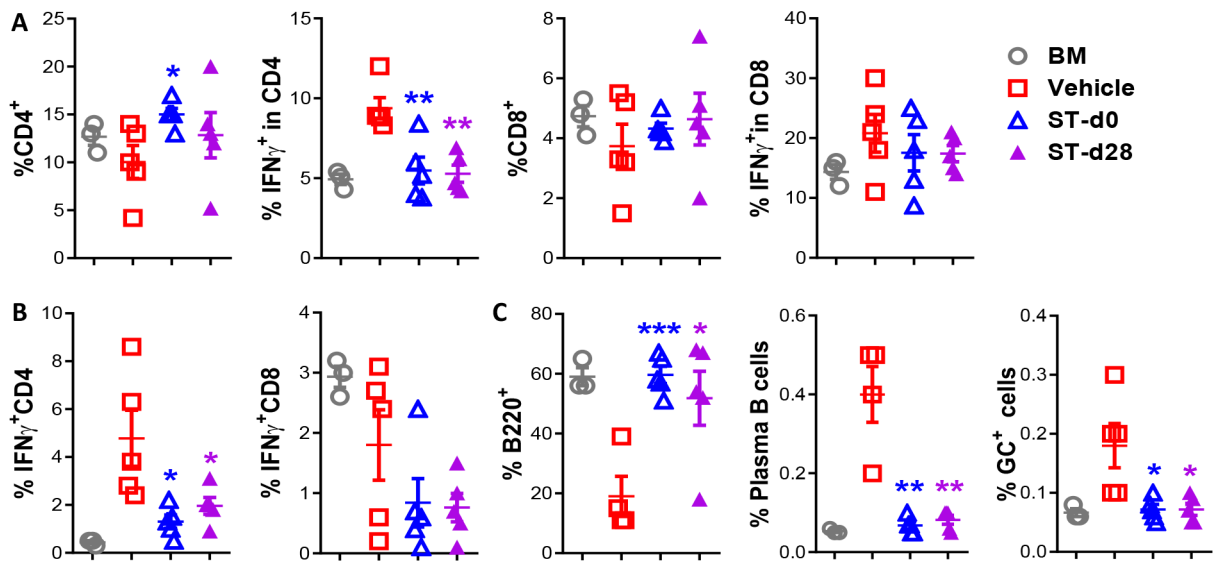


**Figure 2. ST1072 modulates B- and T-cell functions during cGVHD development.**

BALB/c mice were lethally irradiated and  $5 \times 10^6$ /mouse TCD-BM or plus  $5 \times 10^6$ /mouse splenocytes from B10.D2 donor mice were transplanted. One group of the recipient mice was injected i.p. with ST1072 at 2 mg/kg from day-1 to day 28 or day 28 to day 59. The recipients were monitored for body weight and clinical score until 60 days post-BMT. 60 days post cell transfer, spleens and peripheral lymph nodes (pLNs) were collected from the recipient mice and subjected to cell counting and FACS staining. Percentage of CD4<sup>+</sup> or CD8<sup>+</sup> among donor cells and percentage of IFN- $\gamma$  among CD4<sup>+</sup> or CD8<sup>+</sup> donor cells are shown in recipient spleens (A) or periphery lymph nodes (pLNs) (B). Percentages of B220<sup>+</sup> or B220<sup>low</sup>CD138<sup>+</sup> and FAS<sup>+</sup>GL<sup>+</sup> (germinal center cell, GC cell) are shown among donor B cells in recipient spleens (C). Pooled data is summarized with statistical analyses where either treatment (day 0 or 28) was compared with vehicle control. Data shown is one of the two replicate experiments. Significance is determined by one-way ANOVA (using multiple comparison test). Asterisks indicate statistical significance \* $p < 0.05$ , \*\* $p < 0.01$ , \*\*\* $p < 0.001$ .

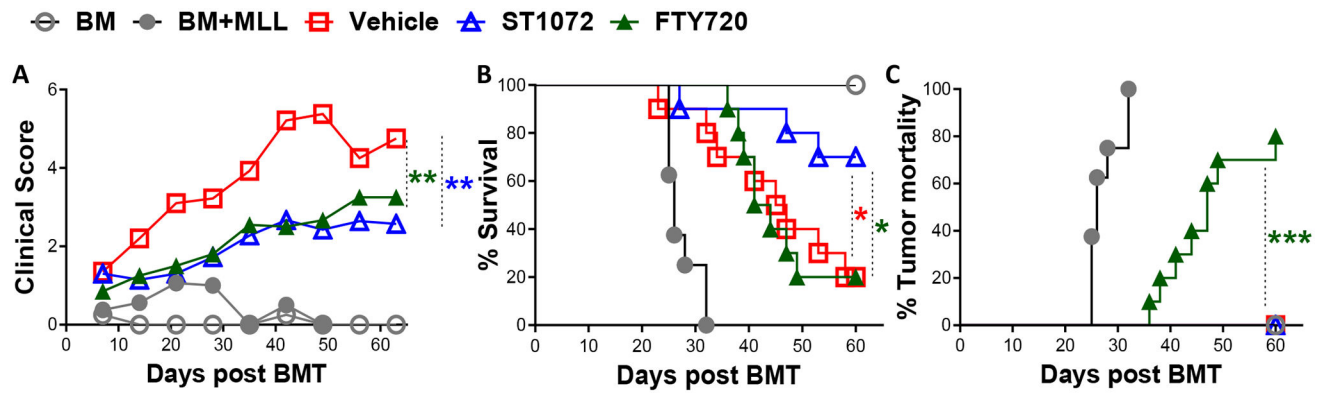


**Figure 3. The effects of ST1072 or FTY720 on GVH and GVL responses.**

BALB/c mice were lethally irradiated and transplanted with  $5 \times 10^6$ /mouse TCD-BM (Ly5.1<sup>+</sup>) or plus purified T cells ( $1 \times 10^6$ ) from B6 mice and mixed-lineage leukemia (MLL) as well. The recipient mice were injected i.p. with ST1072 or FTY720 at 1mg/kg per mouse/day from day -1 to day 14. The mice were monitored for clinical score (A) survival (B) and tumor mortality (C). Data shown here is from two independent experiments (n=10 per group). For comparison of recipient survival and tumor mortality among groups, the log-rank test was used to determine statistical significance. Clinical scores were compared using a nonparametric Mann-Whitney *U* test. Asterisks indicate statistical significance \**p* < 0.05, \*\**p* < 0.01, \*\*\**p* < 0.001.

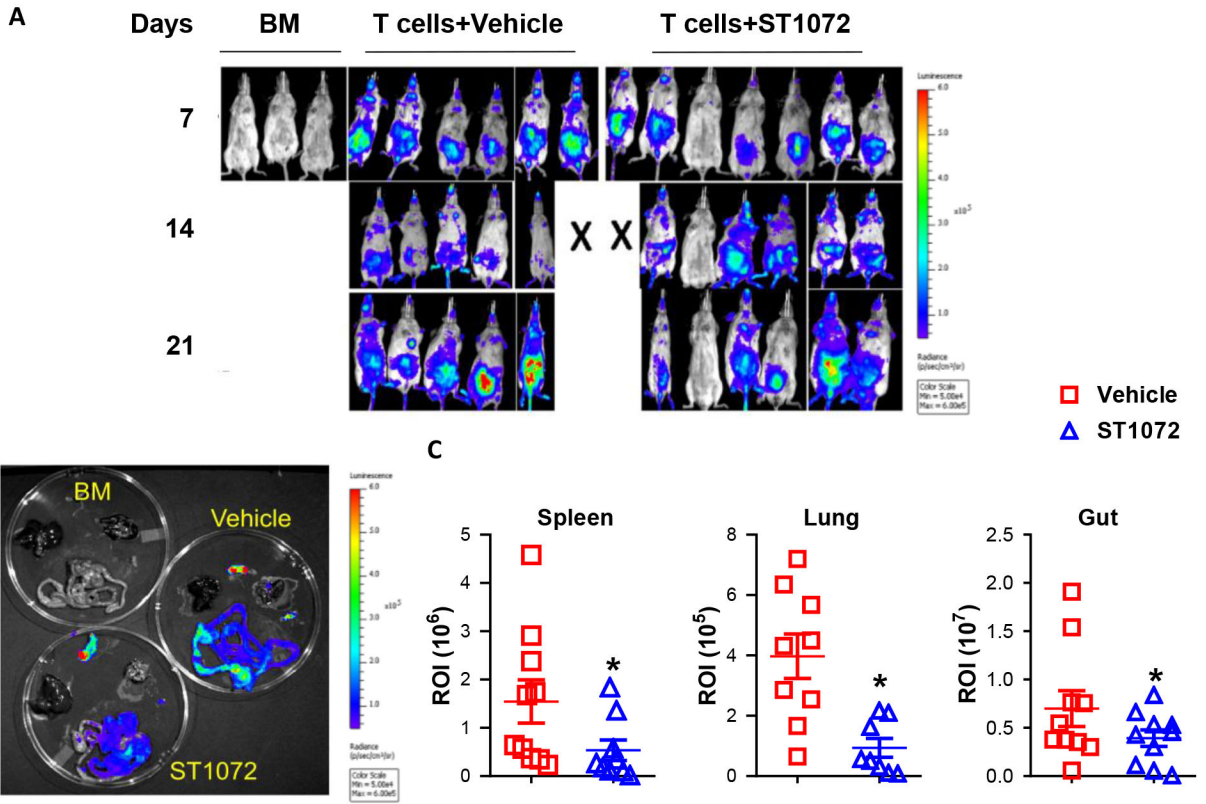


**Figure 4. ST1072 treatment modulates T-cell expansion and migration after allo-BMT.** BALB/c mice were lethally irradiated and transplanted with  $5 \times 10^6$ /mouse TCD-BM (Ly5.1<sup>+</sup>) or plus purified T cells ( $1 \times 10^6$ ) from  $\beta$ -actin luciferase transgenic B6 mice. The recipient mice were injected i.p. with vehicle alone or ST1072 at 1 mg/kg daily from day -1 to day 14. Donor T-cell expansion and migration were monitored using bioluminescent imaging (BLI) at the time points indicated. Macro-photos are shown for BLI of total body (A) and individual organs (B) with a region of interest (ROI) summary (C). Data shown here is pooled from two independent experiments (n=10 per group). Significance is determined by Student's *t* test. Asterisks indicate statistical significance \**p* < 0.05.



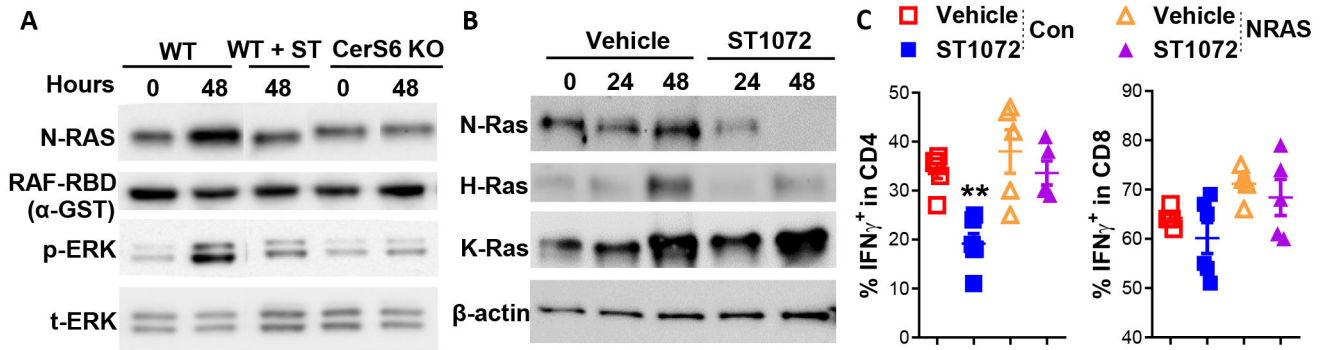


**Figure 5. The role of CerS6 in proximal TCR signaling.**

(A) Freshly isolated T cells from WT or CerS6KO mice were either left unstimulated or stimulated with plate bound anti-CD3 at the time points indicated. Some WT T cells were also stimulated in the presence of ST1072 at 50ug/ml. These T cells were subjected to immunoprecipitation using GST-RAF RBD. Protein lysates were incubated with GST-RAF RBD conjugated glutathione sepharose beads. The proteins bound to the Glutathione beads (top 2 panels) were analyzed by Western blot using anti-NRAS or anti-GST antibodies. Cell lysates were also measured for total or phosphor-ERK antibodies. (B) Freshly isolated T cells from WT mice were stimulated in presence and absence of ST1072 at the time points indicated. The membrane and cytosolic fraction were isolated from these cells and were subjected to western blot analysis for NRAS, H-RAS, K-RAS and  $\beta$ -actin. Data shown here is from one of two independent experiments. The control or oncogenic NRAS (Q61K) plasmid DNA were transfected into naïve T cells using Amaxa Nucleofector kit V from Lonza per manufacturer's instructions. Six hours after, the cells collected and co-cultured with allogeneic antigen presenting cells for 5 days in presence or absence of ST1072. Cultured cells were re-stimulated with PMA/Ionomycin for 4hrs and analyzed for the percentage of IFN- $\gamma$  production on gated CD4<sup>+</sup> or CD8<sup>+</sup> cells (C). Data shown is one of the two replicate experiments. Significance is determined by Student's *t* test. Asterisks indicate statistical significance \*\**p* < 0.01.

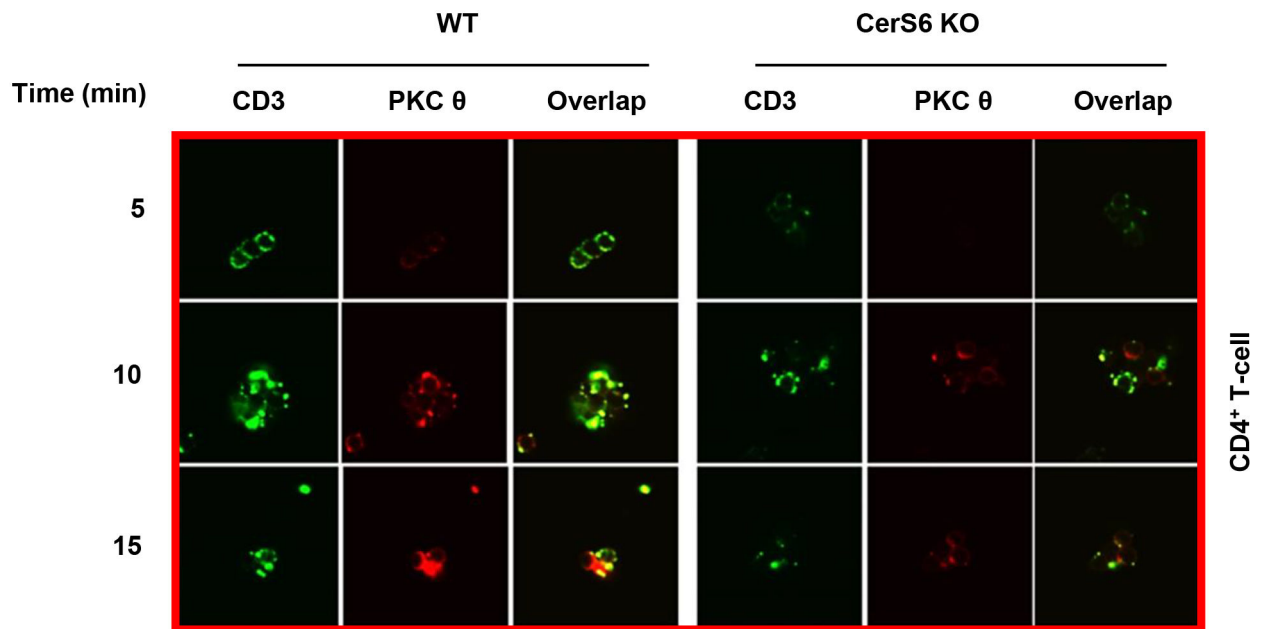


**Figure 6. The effect of CerS6 on CD3 and PKCθ capping in CD4 T cells after TCR stimulation.** Primary CD4 T cells ( $1 \times 10^6$  cells) were engaged with TCR for the indicated time points followed by their incubation with anti-CD3 antibody for 30 minutes at 4°C. After PBS wash and incubation with goat anti-hamster IgG at 37°C, the reaction was stopped immediately, and the cells were washed and incubated with Alexa Fluor 488-conjugated antibody for 30 minutes at 4°C. The cells were fixed and permeabilized followed by incubation overnight at 4°C with PKCθ antibody, and then stained with Alexa Fluor 594 secondary antibody followed by analysis with confocal microscopy (original magnification  $\times 63$ ). At least 6–7 fields in each condition per experiment were examined. The data shown here is one representative of two independent experiments.

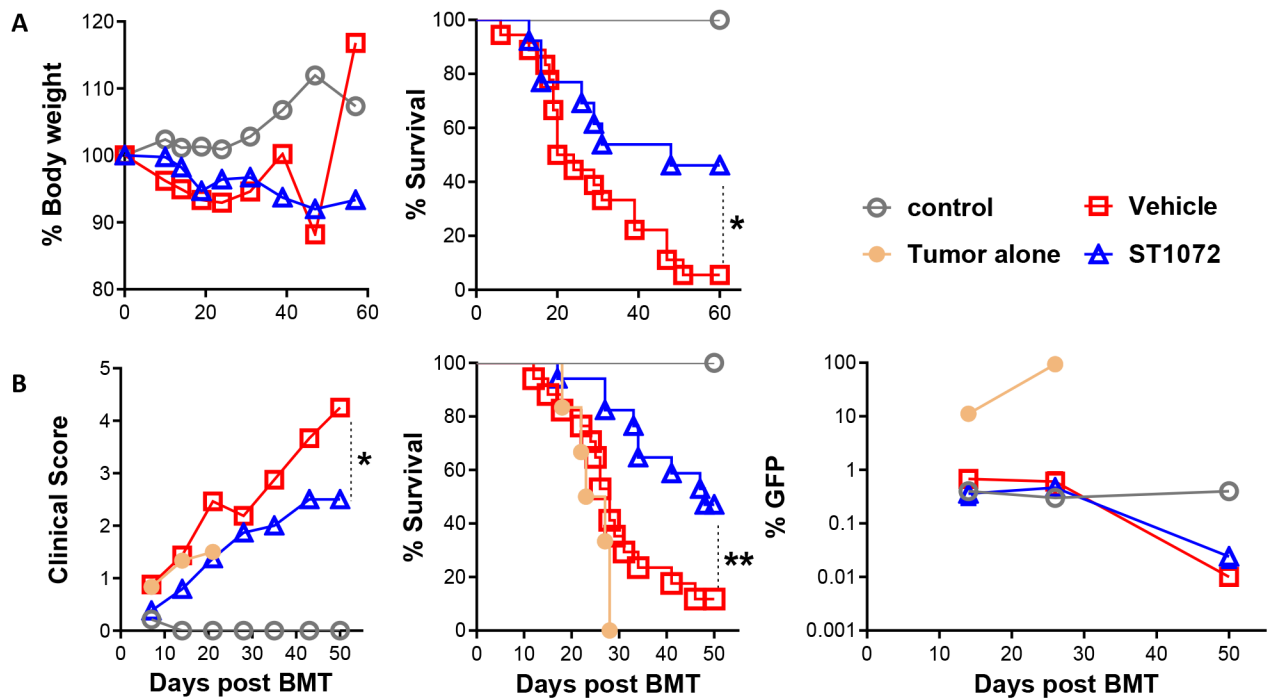


**Figure 7. Preventative treatment with ST1072 reduces GVHD in NSG xenograft mouse model.** NSG-A2<sup>+</sup> mice were irradiated (250 cGy) and were transplanted with HLA-A2<sup>-</sup> human PBMCs ( $10 \times 10^6$ ). The recipient mice were injected i.p. with vehicle or with ST1072 at 1mg/kg daily from day -1 to day 14. The recipients were monitored for body weight and survival (A) until 60 days post transplantation. Data shown here are pooled from two combined experiments (n=13–14 per group). In a separate experiment, Raji B cell lymphoma ( $1 \times 10^6$ ) were infused together with or without HLA-A2<sup>-</sup> human PBMCs ( $10 \times 10^6$ ) into NSG-A2<sup>+</sup> mice, which were treated with vehicle alone or with ST1072. The mice were monitored for clinical score, survival and tumor burden (B) until 50 days post transplantation. Data shown here are from two combined experiments (n=13–14/group). For comparison of recipient survival among groups, the log-rank test was used to determine statistical significance. Clinical scores were compared using a nonparametric Mann-Whitney *U* test. Asterisks indicate statistical significance \**p* < 0.05, \*\**p* < 0.01.

**Table 1.**  
**Association of sphingolipid levels and GVHD development.**

Plasma samples from 17 patients without GVHD and 20 patients with GVHD were measured for the sphingolipids including C14-, C16- and C26- ceramide as well as dhSph-1P and Sph-1P. The levels of each sphingolipid were shown as mean±SD (95%CI). Based on the average level of individual sphingolipid, total 37 patients were divided into high or low expression group. Logistic regression analysis was used to evaluate overall risk (OR) values and related P values, where  $p < 0.05$  indicates significant difference.

	Target	No GVHD--Mean±SD (95%CI)	GVHD--Mean±SD (95%CI)	OR value	P value
<b>GVHD</b>	C14 ceramide	2.81±0.21 (3.35,3.26)	3.91±0.32 (3.26,4.61)	2.241	0.234
	C16 ceramide	43.01±4.00 (34.54,51.48)	82.26±12.52 (52.62,105.72)	24.000	<b>0.005</b>
	C26 ceramide	3.94±0.54 (2.79,5.08)	8.12±1.45 (5.04,11.19)	4.667	0.058
	dhSph-1P	11.76±1.06 (9.50,14.02)	23.69±3.69 (15.87,31.50)	11.250	<b>0.006</b>
	Sph-1P	51.00±4.45 (41.56, 60.44)	87.98±9.62 (67.59, 108.36)	10.889	<b>0.003</b>
<b>Gut GVHD</b>	C14 ceramide	2.91±0.22 (2.43,3.38)	3.92±0.30 (3.29,4.55)	1.746	0.403
	C16 ceramide	44.89±4.21 (36.01,53.77)	82.67±12.05 (57.26,108.09)	11.000	<b>0.007</b>
	C26 ceramide	4.46±0.73 (2.92,6.00)	7.47±1.35 (4.61,10.32)	3.150	0.116
	dhSph-1P	14.53±2.95 (8.31,20.74)	20.95±2.68 (15.29,26.61)	6.875	<b>0.014</b>
	Sph-1P	56.67±7.05 (41.79,71.54)	82.79±8.28 (65.31,100.27)	7.583	<b>0.007</b>
<b>Skin GVHD</b>	C14 ceramide	2.73±0.30 (2.01,3.44)	3.44±0.27 (2.80,4.07)	0.643	0.590
	C16 ceramide	41.14±3.53 (32.80,49.48)	67.83±11.18 (41.39,91.26)	2.222	0.326
	C26 ceramide	4.29±0.83 (2.32,6.26)	5.88±1.10 (3.28,8.47)	0.545	0.501
	dhSph-1P	10.31±1.10 (7.70,12.92)	21.49±6.77 (5.48,31.49)	1.900	0.427
	Sph-1P	48.60±5.62 (35.30,61.90)	72.14±14.60 (31.61,106.66)	1.231	0.795
<b>Liver GVHD</b>	C14 ceramide	2.81±0.21 (3.35,3.26)	3.91±0.32 (3.26,4.61)	2.241	0.234
	C16 ceramide	43.01±4.00 (34.54,51.48)	82.26±12.52 (52.62,105.72)	24.000	<b>0.005</b>
	C26 ceramide	3.94±0.54 (2.79,5.08)	8.12±1.45 (5.04,11.19)	4.667	0.058
	dhSph-1P	11.76±1.06 (9.50,14.02)	23.69±3.69 (15.87,31.50)	11.250	<b>0.006</b>
	Sph-1P	51.00±4.45 (41.56, 60.44)	87.98±9.62 (67.59, 108.36)	10.889	<b>0.003</b>